Magnetic Origin of Giant Magnetoelectricity in Doped Y-type Hexaferrite $Ba_{0.5}Sr_{1.5}Zn_2(Fe_{1-x}Al_x)_{12}O_{22}$

Woo-Suk Noh,[1] Kyung-Tae Ko,[1,2,3] Sae Hwan Chun,[4] Kee Hoon Kim,[4] Byeong-Gyu Park,[5] Jae-Young Kim,[5] and Jae-Hoon Park[1,2,6,*]

[1]*c_CCMR and Department of Physics, Pohang University of Science and Technology, Pohang 790-784, Republic of Korea*
[2]*Max Planck POSTECH Center for Complex Phase Materials, Pohang University of Science and Technology, Pohang 790-784, Republic of Korea*
[3]*Max Planck Institute for Chemical Physics in Solid, 01187 Dresden, Germany*
[4]*FPRD, Department of Physics and Astronomy, Seoul National University, Seoul 151-747, Republic of Korea*
[5]*Pohang Accelerator Laboratory, Pohang University of Science and Technology, Pohang 790-784, Republic of Korea*
[6]*Division of Advanced Materials Science, Pohang University of Science and Technology, Pohang 790-784, Republic of Korea*

(Received 8 December 2014; published 19 March 2015)

We investigated site-specific magnetic behaviors of multiferroic $Ba_{0.5}Sr_{1.5}Zn_2(Fe_{1-x}Al_x)_{12}O_{22}$ using Fe $L_{2,3}$-edge x-ray magnetic circular dichroism. The Al dopants mostly replace the Fe^{3+} ions at octahedral (O_h) sites, which contribute unquenched angular momenta through off-centering displacements. This replacement greatly reduces the magnetic anisotropy energy to change the magnetic order from a helical to a heliconical type with enhanced magnetoelectric susceptibility (α_{ME}). The tetrahedral (T_d) Fe sites exhibit magnetic hysteresis distinguishable from that of the O_h sites, especially at low magnetic fields. These results provide essential clues for the heliconical order with a giant α_{ME} and multibit memory effects in the Al-doped Y-type hexaferrite.

DOI: 10.1103/PhysRevLett.114.117603 PACS numbers: 77.80.-e, 75.30.Gw, 75.60.Ej, 78.70.Dm

Multiferroic materials, in which magnetism and ferroelectricity coexist with a cross coupling, the so-called magnetoelectric (ME) effect, have been intensively studied experimentally and theoretically over the past decade due to their potential technological applications as next-generation multibit memory devices [1–3]. The ME effect was demonstrated in various multiferroic materials such as chromates, manganites, ferrites, etc. [1–6], and spiral, cycloidal, or noncollinear helical magnetic orders were known to be essential for a large ME effect [7–11]. Multiferroicity is well explained by an inverse Dzyaloshinskii-Moriya interaction [12,13] or a spin-current model [14]. However, most of the materials were recognized to face the difficulty of application barriers due to the low ME response, low ME temperature, and/or the requirement of a high magnetic field. Recently, hexaferrites with several different types have attracted much attention as candidates for possible multiferroic application materials with a giant ME susceptibility (α_{ME}) at a relatively high temperature [4,15–17], and even nonvolatile multistate behaviors were demonstrated at room temperature [18]. Particularly in Y-type hexaferrites $(Ba,Sr)_2Zn_2Fe_{12}O_{22}$, small Al doping greatly enhances α_{ME} at a low magnetic field [16].

Y-type hexaferrites $Ba_{0.5}Sr_{1.5}Zn_2(Fe_{1-x}Al_x)_{12}O_{22}$ are crystallized in a stacked hexagonal structure at a $R\bar{3}m$ space group [19,20] with spinel structured blocks consisting of octahedral (O_h) and tetrahedral (T_d) Fe sites as shown in Fig. 1(a). The magnetic structure is conventionally described in terms of alternative stacked L and S blocks with large and small magnetic moments, respectively [4,20]. The magnetic ordering temperatures were reported to be 337 K for $x = 0.00$ and 263 K for $x = 0.08$ [16]. The spin structures are schematically depicted in Fig. 1(b). For $x = 0.00$, both L and S block spins are aligned in a helical order under an in-plane magnetic field $H \| ab$ (~1 T) [20]. The ferroelectricity was

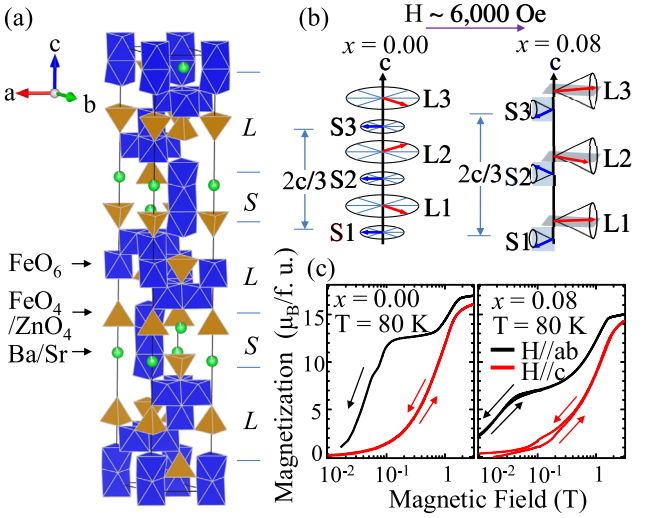

FIG. 1 (color online). (a) Crystal structure of Y-type hexaferrite. (b) Spin structures of $Ba_{0.5}Sr_{1.5}Zn_2(Fe_{1-x}Al_x)_{12}O_{22}$ for $x = 0.00$ and 0.08 at $H = 6000$ Oe. (c) M vs H curves.

 © 2015 American Physical Society

proposed to be induced by an inversion symmetry breaking [4]. Meanwhile, for $x = 0.08$, the spin order changes into a heliconical type with a certain c-direction magnetic component in the S block under $H\|ab$ [16,21,22]. The cone-shaped spin blocks lead ferroelectricity with a greatly enhanced α_{ME} through the spin-current mechanism katsura. The change in the spin structure was attributed to reduction of the in-plane magnetic anisotropy energy [15–17]. Indeed, the difference between the in-plane and out-of-plane magnetizations decreases with the doping in a 0.1–1 T region as shown in Fig. 1(c). Moreover, one can also recognize a certain in-plane remanent magnetization for $x = 0.08$, which is essential for multibit memory device applications [15,18].

In this Letter, we performed x-ray magnetic circular dichroism (XMCD) measurements on the Y-type hexaferrites $Ba_{0.5}Sr_{1.5}Zn_2(Fe_{1-x}Al_x)_{12}O_{22}$ ($x = 0.00,\ 0.08$) to explore a microscopic origin for the changes in the magnetic behavior with the doping and to find out a clue for the remanent magnetization. The results show unquenched orbital magnetic moments for both $x = 0.00$ and 0.08. The orbital moment m_o, which is mostly induced from off-centered octahedral (O_h) Fe sites, is reduced with the doping, resulting in a decrease of the in-plane magnetic anisotropy energy to change the spin structure with a largely enhanced α_{ME}. We also determined site-specific magnetic hystereses for the O_h and T_d Fe sites. The T_d site hysteric behavior is distinguishable from that of the O_h site with Al doping and originates a certain increase of remanent magnetization for the multistate behavior.

$Ba_{0.5}Sr_{1.5}Zn_2(Fe_{1-x}Al_x)_{12}O_{22}$ ($x = 0.00,\ 0.08$) single crystals were grown by a flux method. Samples were cleaved *in situ* in a vacuum better than 5×10^{-10} Torr. XMCD measurements were performed at the 2*A* soft x-ray elliptically polarized undulator beam line in Pohang Light Source. The results were obtained at 80 K with ~95% circularly polarized light. A 0.5 T electromagnet was used for magnetization switching, the photon incident angle is 22.5° off from the H direction ($H\|c$ or $H\|ab$), and XMCD spectra were collected in the total electron yield mode. The magnetization data were obtained by using a Quantum Design physical property measurement system.

To explore magnetic anisotropy of the system, we performed Fe $L_{2,3}$-edge XMCD measurements. The net spin moment direction was flipped to be parallel (ρ_+) and antiparallel (ρ_-) to the photon helicity vector at each data point. The spectra were averaged over right and left helicities to minimize artificial effects. Figures 2(a) and 2(b) present the results of the absorption spectra (ρ_+ and ρ_-), dichroisms ($\Delta\rho = \rho_+ - \rho_-$), and integrations [$\int(\Delta\rho)dE$] of the undoped ($x = 0.00$) and Al-doped ($x = 0.08$) samples, respectively. The degree of circular polarization and the geometry factor were taken into account in the spectra. The spectra are roughly divided into the L_3 ($2p_{3/2}$) and L_2 ($2p_{1/2}$) regions. The integrations

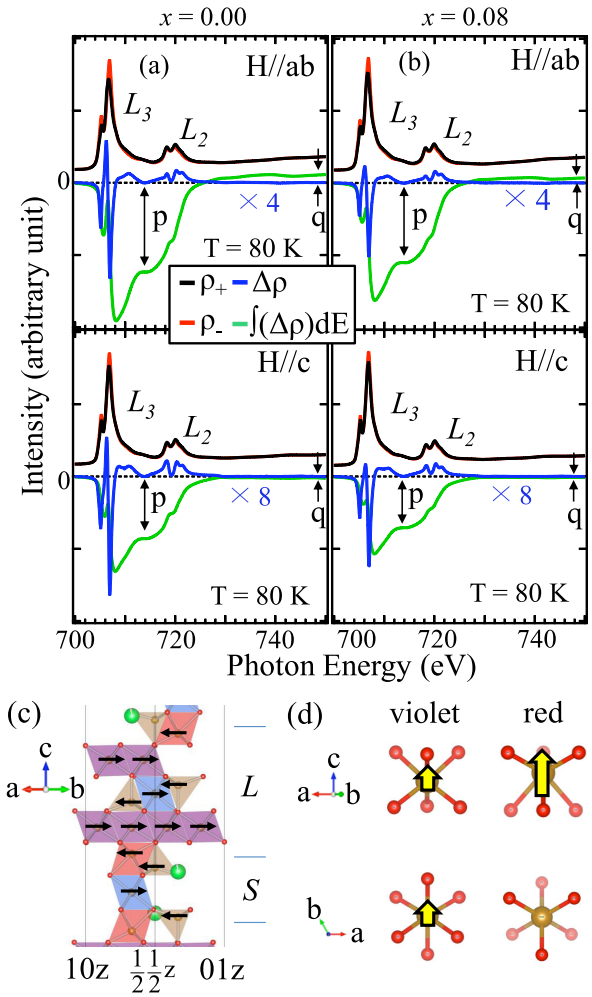

FIG. 2 (color online). Fe L-edge XMCD results of Y-type hexaferrite $Ba_{0.5}Sr_{1.5}Zn_2(Fe_{1-x}Al_x)_{12}O_{22}$ at $T = 80$ K, $H = 6000$ Oe for (a) $x = 0.00$ and (b) $x = 0.08$ under $H\|ab$ (top) and $H\|c$ (bottom). (c) Spin configurations of Fe^{3+} polyhedra under a saturation in-plane H field. (d) Off-centering displacements of Fe^{3+} in two different O_h sites.

over L_3 and entire $L_{2,3}$ regions are presented with p and q, which are roughly proportional to the spin and orbital magnetic moments m_s and m_o, respectively [23]. The obtained p values are consistent with the magnetizations at 80 K under $H = 6000$ Oe. Using the sum rule [23], we estimated the orbital to spin moment ratio $m_o/m_s = 2q/(9p - 6q) = -0.018$ for $H\|ab$ (H_{ab}) and $m_o/m_s = +0.0046$ for $H\|c$ (H_c). As the spins are fully aligned (eight up- and four down-spin Fe^{3+} ions) [4,20], the ionic magnetic moment becomes $20\mu_B$/f.u. (~10% larger than the saturated moment M_S at 10 K), and $m_o = -0.38\mu_B$/f.u. for H_{ab} and $m_o = +0.09\mu_B$/f.u. for H_c, resulting in in-plane magnetic anisotropy. There exist only half-filled Fe^{3+} ($L = 0$, $S = 5/2$) ions, and off-centering displacements can be considered as the origin of the nonvanishing m_o as discussed in $GaFeO_3$ [24]. Indeed, one can find the off-centering distortions in the Y-type hexaferrite [19,25].

Figure 2(c) shows the arrangement of $(Fe,Zn)O_4$ (T_d) and FeO_6 (O_h) polyhedra in the undoped hexaferrite with four T_d sites (brown) and ten O_h sites per formula unit (f.u.). The O_h sites are classified into three different groups presented with three different colors (two red, six violet, and two blue O_h sites) in the figure. The T_d sites are distributed with two Zn^{2+} and two Fe^{3+} ions, while all the O_h sites are occupied by Fe^{3+} ions. The L block contains two T_d sites (~0.67 Fe^{3+}) and nine O_h sites (two reds, six violets, and one blue), and the S block has two T_d sites (~1.33 Fe^{3+}) and one O_h site (blue) [20,26]. The spin directions are presented with black arrows for H_{ab}. A large off-centering displacement occurs along the c axis at the red O_h site, while at the violet O_h site a small off-centering displacement does both along the c axis and in the ab plane, as depicted with thick arrows in Fig. 2(d). The off-centering is negligible at the T_d and blue O_h sites. The shortest to average Fe-O bond length ratio within an FeO_6 octahedron is 0.93 for the red and 0.98 for the violet [25], indicating that the obtained in-plane $m_o = -0.38\mu_B$/f.u. mostly comes from the two red sites. The magnitude of m_o is comparable to that of $GaFeO_3$ with the ratio of 0.92 [24,27]. Considering that the orbital angular momentum is parallel to the spin momentum in an Fe^{3+} [24], its negative sign results from the red site spin direction opposite to the net M direction. Meanwhile, a smaller out-of-plane $m_o = +0.09\mu_B$/f.u. is mainly from the six violet sites with the spin direction parallel to the M direction.

The Al doping largely reduces the in-plane magnetic anisotropy. For $x = 0.08$, the ratio was obtained to be $m_o/m_s = -0.013$ under $H_{ab} = 6000$ Oe and $m_o/m_s = +0.0044$ under $H_c = 6000$ Oe from the XMCD results. The Al dopants were known to mostly replace the O_h sites [16]. By supposing that those are uniformly distributed only at the O_h sites, the ionic magnetic moment becomes $17.1\mu_B$/f.u., and $m_o = -0.22\mu_B$/f.u. for H_{ab} and $m_o = +0.06\mu_B$/f.u. for H_c, resulting in about 40% reduction in the magnetic anisotropy energy. This reduction is responsible for the spin structure change from a helical to a heliconical order [Fig. 1(b)]. One may notice that the reduction in m_o is rather large in comparison with the 0.08 doping rate, which increases up to 9.6% in average under the assumption of all Al dopants at the O_h sites. This large reduction can be attributed to two factors: (i) a certain decrease of the off-centering displacement with a reduction of the c lattice constant and (ii) a preference of the Al replacement for the red O_h site [28]. A recent nuclear magnetic resonance study reported that the Al replacement rate at the off-centered O_h site (red) is considerably larger than the rate at the other O_h sites (violet and blue) [29].

Besides the variations in m_o/m_s, the MCD spectral line shape also varies with the H-field direction and the Al doping. To extract information on the magnetic ordered states, we analyzed the line shapes by using cluster model calculations with full atomic multiplets and configuration interactions, the so-called CI calculations [30]. The calculated MCD spectra for FeO_6 (O_h) and FeO_4 (T_d) are extracted by fitting the MCD spectrum of a ferrimagnet γ-Fe_2O_3 [31], in which the O_h and T_d Fe^{3+} spins are antiferromagnetically ordered with a 5:3 ratio. In the calculations, the spin moments are estimated to be $4.61\mu_B$ and $4.68\mu_B$ for Fe^{3+} at the O_h and T_d sites, respectively, resulting in a maximum spin moment of $18.3\mu_B$/f.u. for $x = 0.00$ [eight O_h up spins and two T_d and two O_h down spins, i.e., a net spin moment of $6 \times m_s(O_h)$ minus $2 \times m_s(T_d)$]. As the ratio $m_o/m_s = -0.018$ is taken into account, the total moment becomes $18.0\mu_B$/f.u., which well agrees with the in-plane saturated moment $M_S = 17.9\mu_B$/f.u. at 10 K.

Figure 3 shows the calculated MCD spectra for the L_3 region, in comparison with the experimental ones, and the spin structures for $x = 0.00$ and $x = 0.08$ at $H_{ab} = 6000$ Oe and $H_c = 6000$ Oe. The variation in the line shape can be reproduced by tuning the O_h to T_d site MCD ratio. Although the spin alignment with the saturated M has the O_h to T_d spin ratio of 3 : −1, the MCD ratio can be vary with the spin structure in the applied H field smaller than the saturation field (>3 T). In the $x = 0.00$ case (undoped), the best fits were obtained with the ratios of 2.3 : −1 and 2.7 : −1 for the H_{ab} and H_c, respectively. For the H_{ab}, the spin structure has a helical order with an in-plane tilting angle ϕ of the L block spin, the so-called intermediate-II phase [4,20], and $\phi \simeq 78°$ is estimated from the ratio 2.3 : −1 and $M \simeq 13\mu_B$/f.u. (76% of $M_S \simeq 17\mu_B$ at 80 K). Meanwhile, H_c tilts the spins to the c direction and produces a conical order. Considering $M \simeq 0.48M_S$ at 80 K, the cone angles are estimated to be $\alpha \simeq 61°$ for the L block spin and the angle $\alpha' \simeq 53°$ for the S block spin. In both spin structures by H_{ab} and H_c, the angle between the L and S block spins is nearly maintained to be ~140°.

In the $x = 0.08$ case (Al doped), the spin structure becomes a heliconical order with a cone angle β for H_{ab}. The MCD ratio is estimated to be 2.8 : −1, which gives a maximum spin moment $16.5\mu_B$/f.u. [a net moment of $5.6 \times m_s(O_h)$ minus $2 \times m_s(T_d)$]. This value is consistent with the observed $M_S = 16.2\mu_B$/f.u., which results in the maximum spin moment $16.4\mu_B$/f.u. with $m_o/m_s = -0.013$. The cone angle is estimated to be $\beta \simeq 48°$ at $H_{ab} = 6000$ Oe from $M = 0.67M_S$ at 80 K. For $H_c = 6000$ Oe, the spin structure becomes the conical order again [see Fig. 3(d)]. The cone angles $\gamma \simeq 67°$ and $\gamma' \simeq 75°$ were estimated from the O_h to T_d ratio of 3.5 : −1 and $M \simeq 0.41M_S$ at 80 K. The angle between the L and S block spins reduces to ~120°.

The L_3 MCD line shape shown in Fig. 4(a) presents typical O_h-T_d Fe^{3+} ferrimagnet features o, t, and o' resulting from a ferrimagnetic order of a large O_h site spin and a small T_d site spin, as in γ-Fe_2O_3 [24]; the features o and o' are due to the O_h site up spin, and t is due to the T_d site down spin as can be seen in Fig. 3. Thus, we

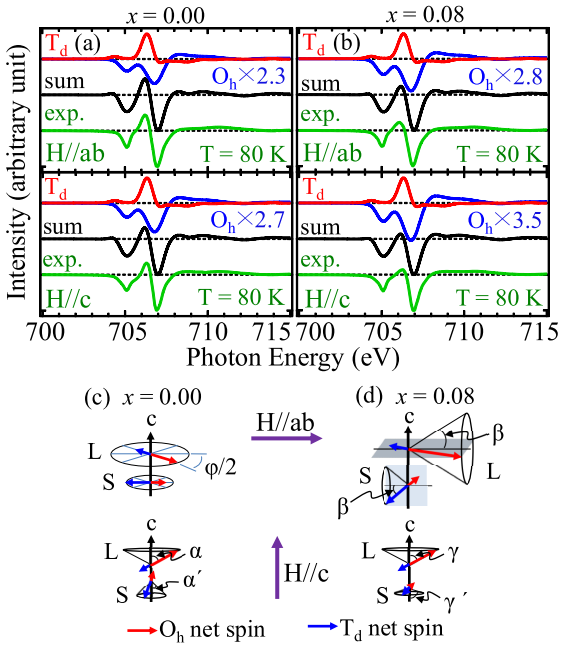

FIG. 3 (color online). Fe L_3-edge MCD spectra obtained from the CI calculations compared with the experimental ones for (a) $x = 0.00$ and (b) $x = 0.08$ in $Ba_{0.5}Sr_{1.5}Zn_2(Fe_{1-x}Al_x)_{12}O_{22}$ at $H\|ab$ and $H\|c$. Spin structures at $H = 6000$ Oe and at 80 K for (c) $x = 0.00$ and (d) $x = 0.08$.

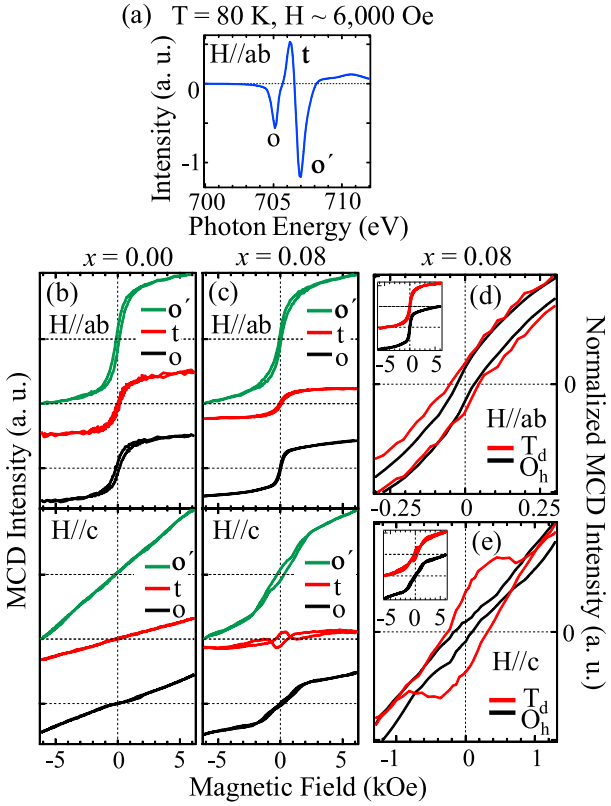

FIG. 4 (color online). (a) Fe L_3-edge MCD spectra of $Ba_{0.5}Sr_{1.5}Zn_2(Fe_{1-x}Al_x)_{12}O_{22}$ ($x = 0.00$). (b),(c) MCD intensities of the three features as a function of H for (b) $x = 0.00$ and (c) $x = 0.08$. Here, the MCD intensity at the feature t is flipped for convenience. (d) Normalized site-specific magnetic hystereses of the O_h and T_d sites determined from effective summations of the H-dependent MCD intensities.

could obtain the site-specific magnetic hysteresis curves by monitoring the MCD peak intensity of each feature as a function of the H field. Figures 4(b) and 4(c) show the $H\|ab$ and $H\|c$ magnetic hysteresis curves of the MCD features for $x = 0.00$ and $x = 0.08$, respectively. In the $x = 0.00$ case, all three features display nearly identical hysteresis behaviors for both H_{ab} and H_c, which coincide with one another with normalization factors corresponding to their different MCD intensities. Meanwhile, in the Al-doped $x = 0.08$ case, the hystereses for the features o and o', which are nearly identical to each other, are somewhat distinguishable from that for the feature t, especially in the low field region $-0.1\ \text{T} < H < 0.1\ \text{T}$, indicating that the magnetic response of the O_h site spin is different from that of the T_d site spin.

The magnetic hystereses for the O_h and T_d site spins can be extracted by taking into account their MCD contributions at the specific photon energies of features o, o', and t obtained from the CI calculation fits as presented in Fig. 3. Figures 4(d) and 4(e) show the normalized site-specific magnetic hystereses for $H\|ab$ and $H\|c$, respectively. Effective summations of these site-specific hystereses well reproduce the observed M-H curves presented in Fig. 1(c) [31]. For $H\|ab$, the T_d site has slightly larger values in the remanent ratio and coercive field, although its overall hysteresis behavior is similar to that of the O_h site. On the other hand, the difference in the hysteresis behavior becomes more remarkable for $H\|c$ with much larger values in the ratio and field at the T_d site. The nonmagnetic Al dopants, which mostly replace the O_h sites, may loosen the magnetic exchange coupling of the neighboring T_d site Fe spins to the O_h site spins to make the magnetic behavior of the T_d site separated from that of the O_h site at the low magnetic field. This separated spin behavior may cause the change of the spin structure from helical to heliconical in the low field region in cooperation with the reduced in-plane magnetic anisotropy energy. As a result, the Al doping largely enhances the low field α_{ME} and increases the remanent magnetization, which is essential for the multibit memory effects demonstrated in the multiferroic hexaferrites [18].

In summary, we reported detailed studies of magnetic origins for improved magnetoelectric effects in the doped Y-type hexaferrite $Ba_{0.5}Sr_{1.5}Zn_2(Fe_{1-x}Al_x)_{12}O_{22}$ using the Fe L-edge XMCD measurements. The Al dopants not only reduce the in-plane magnetic anisotropy energy to change the spin structure from a helical to a heliconical type but also loosen the magnetic coupling between the T_d and O_h sites resulting in distinguishable site-specific magnetic hysteresis behaviors. The results provide essential clues for the enhanced α_{ME} and the multibit memory effects in the Al-doped Y-type hexaferrites.

This work was supported by the National Creative Initiative (No. 2009-0081576 and No. 2010-0018300) and Max Planck POSTECH/KOREA Research Initiative (No. 2011-0031558) programs through NRF funded by MSIP of Korea. PAL is supported by POSTECH and MSIP of Korea.

*To whom all correspondence should be addressed.
jhp@postech.ac.kr

[1] T. Kimura, T. Goto, H. Shintani, K. Ishizaka, T. Arima, and Y. Tokura, Nature (London) **426**, 55 (2003).
[2] B. B. Van Aken, J.-P. Rivera, H. Schmid, and M. Fiebig, Nature (London) **449**, 702 (2007).
[3] S.-W. Cheong and M. Mostovoy, Nat. Mater. **6**, 13 (2007).
[4] T. Kimura, G. Lawes, and A. P. Ramirez, Phys. Rev. Lett. **94**, 137201 (2005).
[5] Y. Tokura and S. Seki, Adv. Mater. **22**, 1554 (2010).
[6] I. A. Sergienko and E. Dagotto, Phys. Rev. B **73**, 094434 (2006).
[7] M. Kenzelmann, A. Harris, S. Jonas, C. Broholm, J. Schefer, S. Kim, C. Zhang, S.-W. Cheong, O. Vajk, and J. Lynn, Phys. Rev. Lett. **95**, 087206 (2005).
[8] G. Lawes *et al.*, Phys. Rev. Lett. **95**, 087205 (2005).
[9] K. Taniguchi, N. Abe, T. Takenobu, Y. Iwasa, and T. Arima, Phys. Rev. Lett. **97**, 097203 (2006).
[10] T. Kimura, Annu. Rev. Mater. Res. **37**, 387 (2007).
[11] H. Jang *et al.*, Phys. Rev. Lett. **106**, 047203 (2011).
[12] I. Dzyaloshinskii, J. Phys. Chem. Solids **4**, 241 (1958).
[13] T. Moriya, Phys. Rev. **120**, 91 (1960).
[14] H. Katsura, N. Nagaosa, and A. V. Balatsky, Phys. Rev. Lett. **95**, 057205 (2005).
[15] S. Ishiwata, Y. Taguchi, H. Murakawa, Y. Onose, and Y. Tokura, Science **319**, 1643 (2008).
[16] S. H. Chun *et al.*, Phys. Rev. Lett. **104**, 037204 (2010).
[17] S. Ishiwata, D. Okuyama, K. Kakurai, M. Nishi, Y. Taguchi, and Y. Tokura, Phys. Rev. B **81**, 174418 (2010).
[18] S. H. Chun *et al.*, Phys. Rev. Lett. **108**, 177201 (2012).
[19] J. Smit and H. P. J. Wijn, in *Ferrites* (Philips' Technical Library, Eindhoven, 1959).
[20] N. Momozawa and Y. Yamaguchi, J. Phys. Soc. Jpn. **62**, 1292 (1993).
[21] H. B. Lee, Y.-S. Song, J.-H. Chung, S. H. Chun, Y. S. Chai, K. H. Kim, M. Reehuis, K. Prokeš, and S. Mat'aš, Phys. Rev. B **83**, 144425 (2011).
[22] H. Chang, H. B. Lee, Y.-S. Song, J.-H. Chung, S. A. Kim, I. H. Oh, M. Reehuis, and J. Schefer, Phys. Rev. B **85**, 064402 (2012).
[23] C. T. Chen, Y. Idzerda, H.-J. Lin, N. Smith, G. Meigs, E. Chaban, G. Ho, E. Pellegrin, and F. Sette, Phys. Rev. Lett. **75**, 152 (1995).
[24] J.-Y. Kim, T. Y. Koo, and J.-H. Park, Phys. Rev. Lett. **96**, 047205 (2006).
[25] A. Collomb, J. Muller, J. C. Guitel, and J. M. Desvignes, J. Magn. Magn. Mater. **78**, 77 (1989).
[26] S. Utsumi, D. Yoshiba, and N. Momozawa, J. Phys. Soc. Jpn. **76**, 034704 (2007).
[27] E. F. Bertaut, G. Bassi, G. Buisson, J. Chappert, A. Delapalme, R. Pauthenet, H. P. Rebouillat, and R. Aleonard, J. Phys. (Paris) **27**, 433 (1966).
[28] From the reduction value in the saturation magnetic moment with the 8% doping, the replacement rate at the red O_h sites is estimated to be about 70% larger than the rates at other O_h sites.
[29] S. Kwon, D. Y. Yoon, S. Lee, Y. S. Chai, S. H. Chun, and K. H. Kim, Phys. Rev. B **88**, 064404 (2013).
[30] A. Tanaka and T. Jo, J. Phys. Soc. Jpn. **63**, 2788 (1994).
[31] See Supplemental Material at http://link.aps.org/supplemental/10.1103/PhysRevLett.114.117603 for additional information, which includes Refs. [24,32,33].
[32] S. Brice-Profeta, M. A. Arrio, E. Tronc, I. Letard, Ch. Cartier dit Moulin, and Ph. Sainctavit, Phys. Scr. T **115**, 626 (2005).
[33] J. Chen, D. Huang, A. Tanaka, C. Chang, S. Chung, W. Wu, and C. Chen, Phys. Rev. B **69**, 085107 (2004).